SUPPLEMENTARY MATERIALS

Sensors to the diagnostic assessment of anticancer and antimicrobial therapies effectiveness by drugs with pyrazine scaffold

Marta Domżalska [1], Aleksandra M. Dąbrowska [1], Dawid Chojnowski [2] and Mariusz Makowski [1,*] Agnieszka Chylewska [1,*]

[1] University of Gdańsk, Faculty of Chemistry, Department of Bioinorganic Chemistry, Wita Stwosza 63, 80-308 Gdańsk, Poland
[2] Keyence International, Irysowa 1, 55-040 Kobierzyce, Bielany Wrocławskie

* Correspondence: agnieszka.chylewska@ug.edu.pl (A.C.); mariusz.makowski@ug.edu.pl (M.M.)

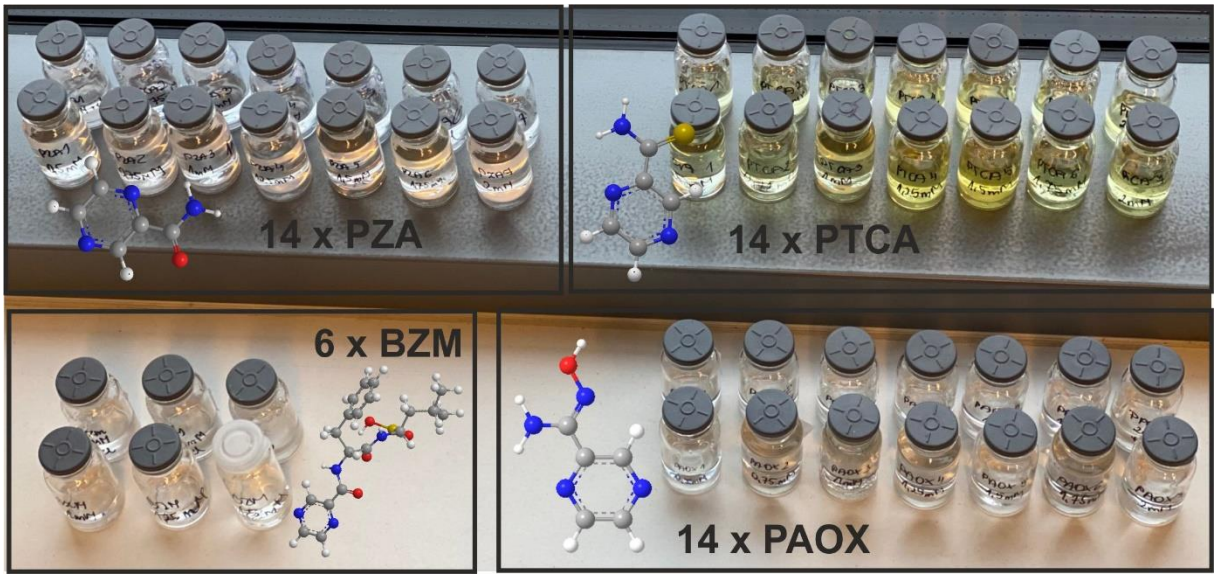

Figure S1. Pyrazine derivatives were prepared in the form of aqueous solutions (concentration range 0.50-2.00 mM with a gradient of 0.25 units) to plot calibration curves used successively for specific tests with the use of polyamine acid GCE sensors.

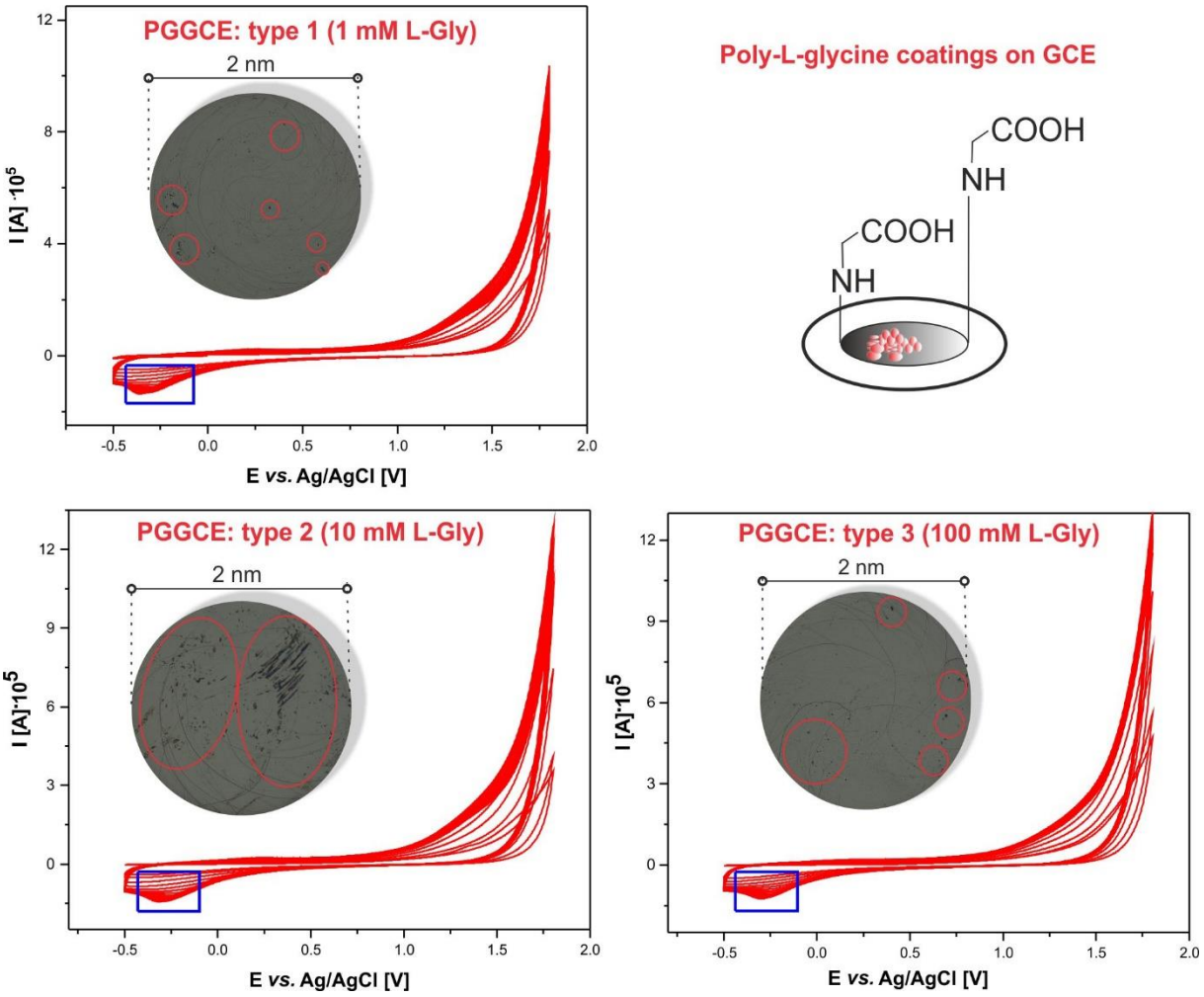

Figure S2. The effects of carrying out the GCE electropolymerization process in three L-Gly modifier systems (areas marked in blue frame indicate a significant range of surfaces with confirmed poly-forms obtained as a result of the modification).

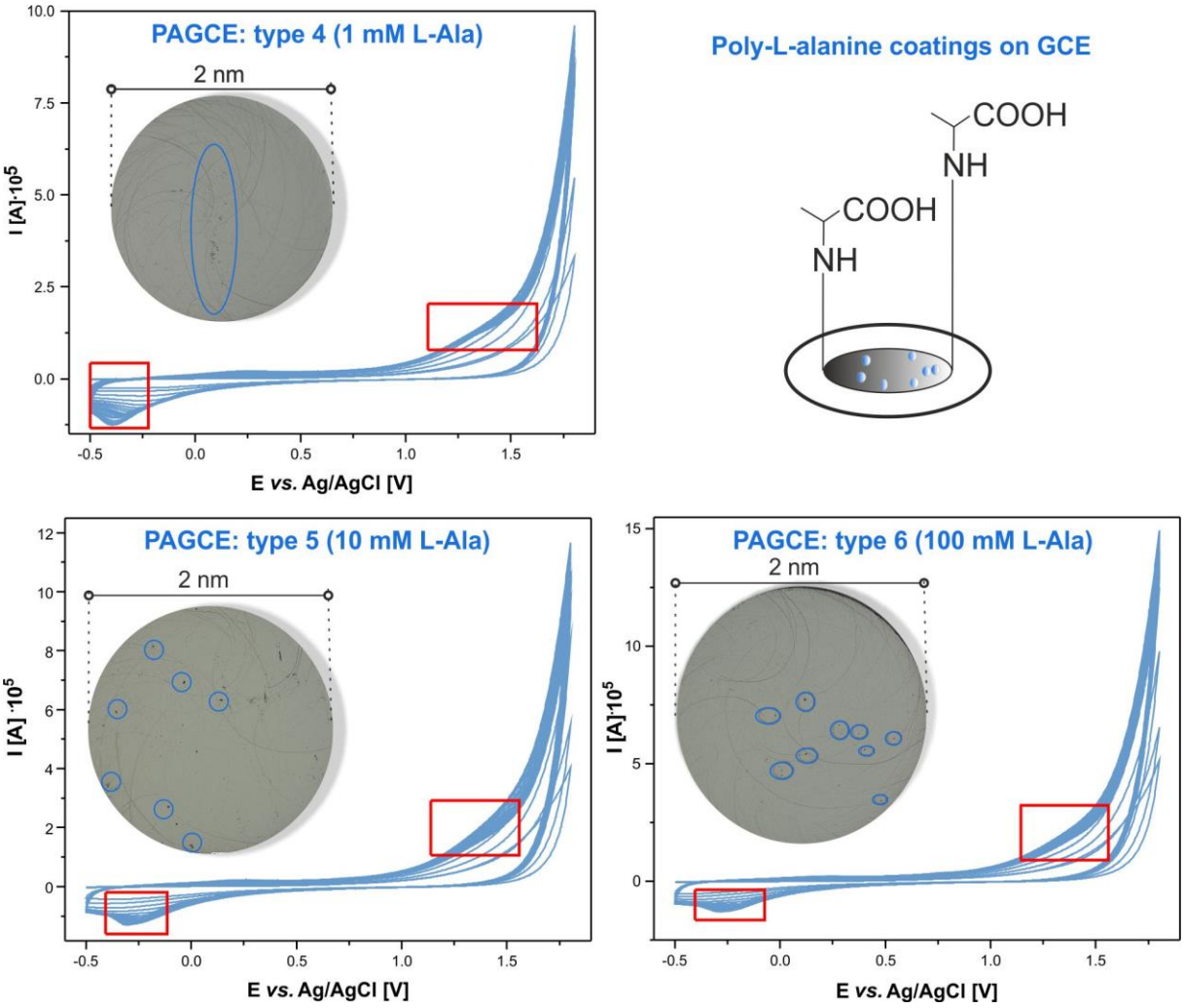

Figure S3. The effects of carrying out the GCE electropolymerization process in three L-Ala modifier systems (areas marked in the red frame indicate a significant range of surfaces with confirmed poly-forms obtained as a result of the modification).

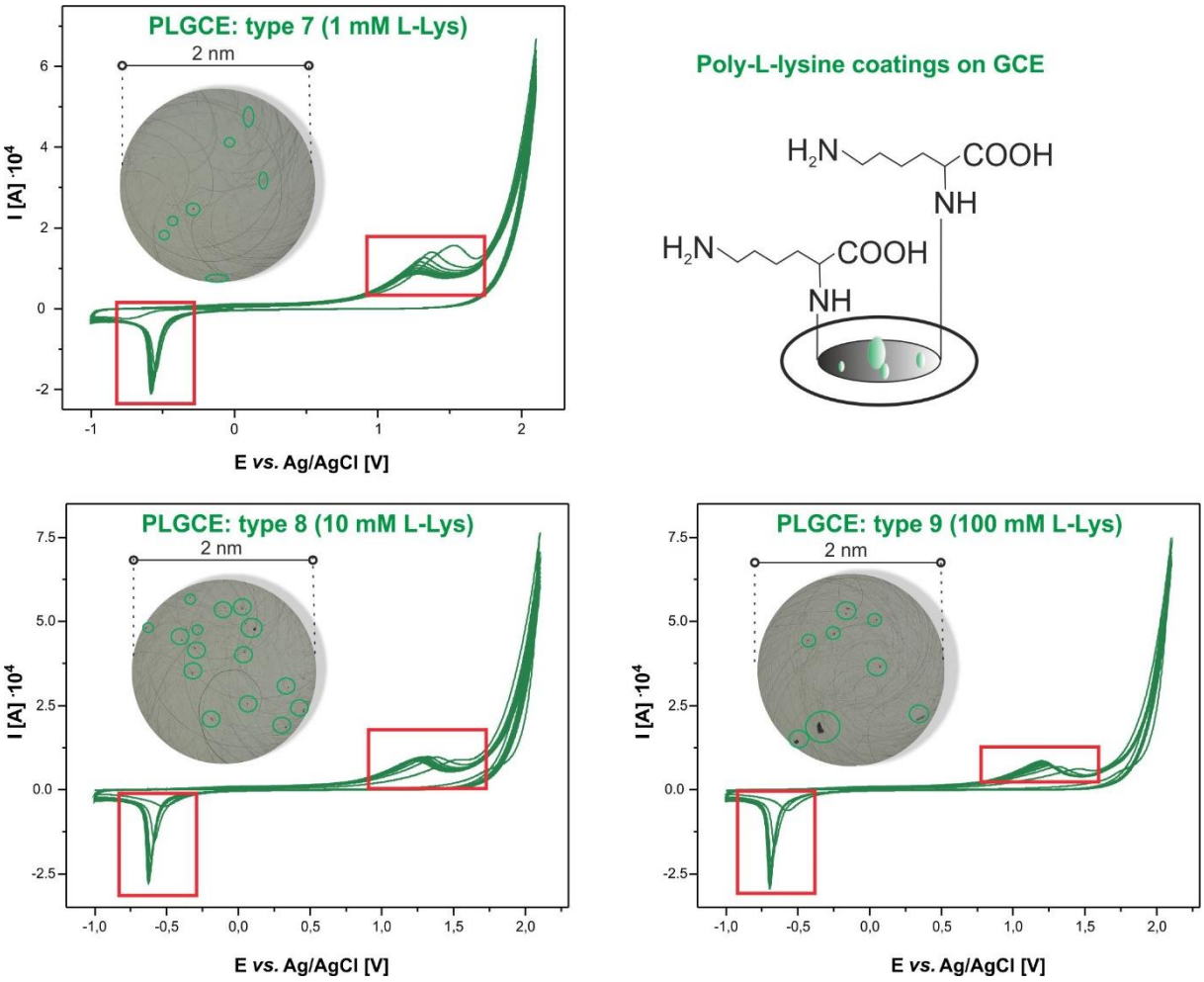

Figure S4. The effects of carrying out the GCE electropolymerization process in three L-Lys modifier systems (areas marked in green frame indicate a significant range of surfaces with confirmed poly-forms obtained as a result of the modification).

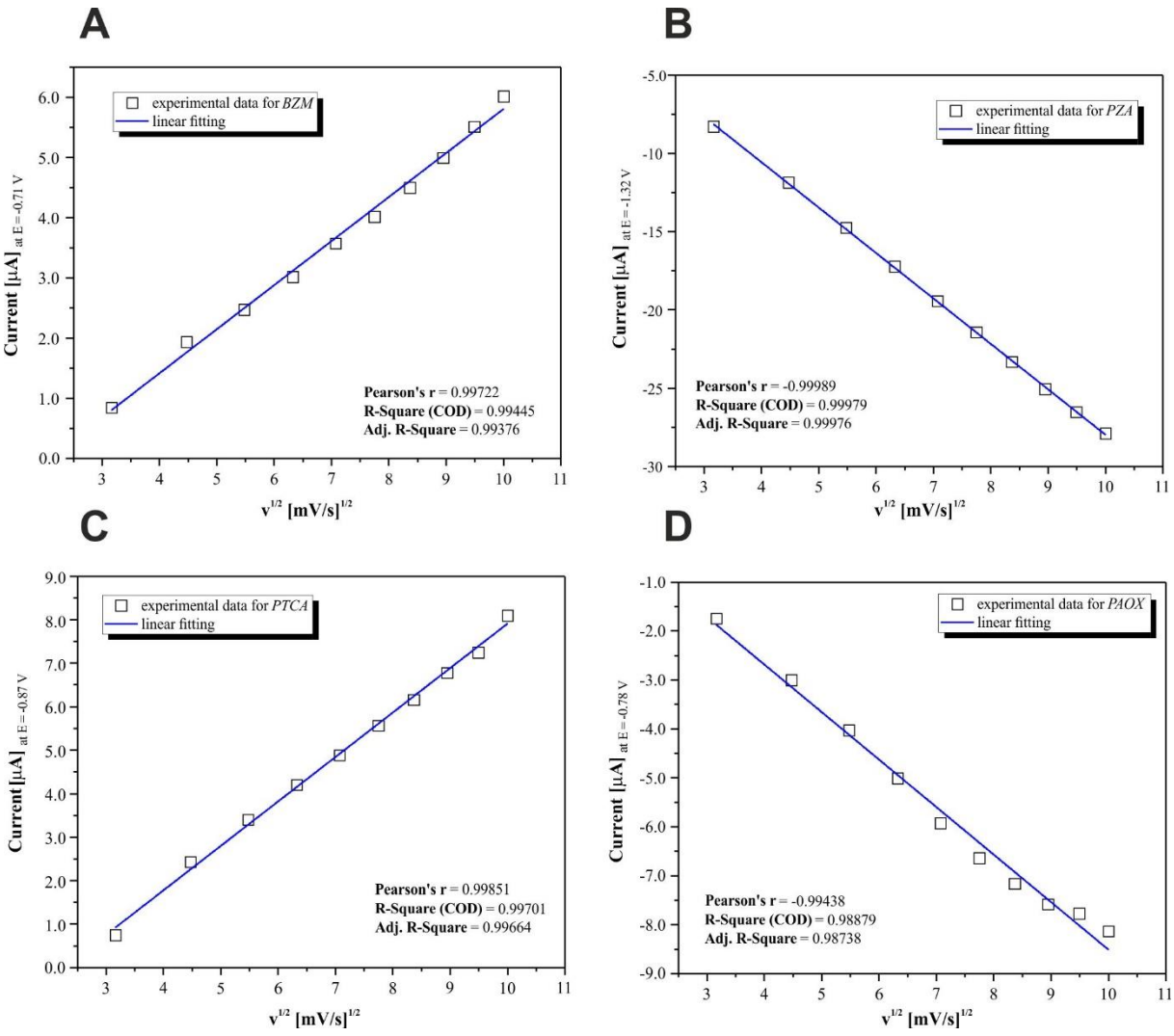

Figure S5. Plots of current peak *vs.* square root of scan rate obtained to prove that electrochemical reaction on GCE is diffusion-controlled in the case of all analytes studied: *BZM* (**A**), *PZA* (**B**), *PTCA* (**C**), *PAOX* (**D**).

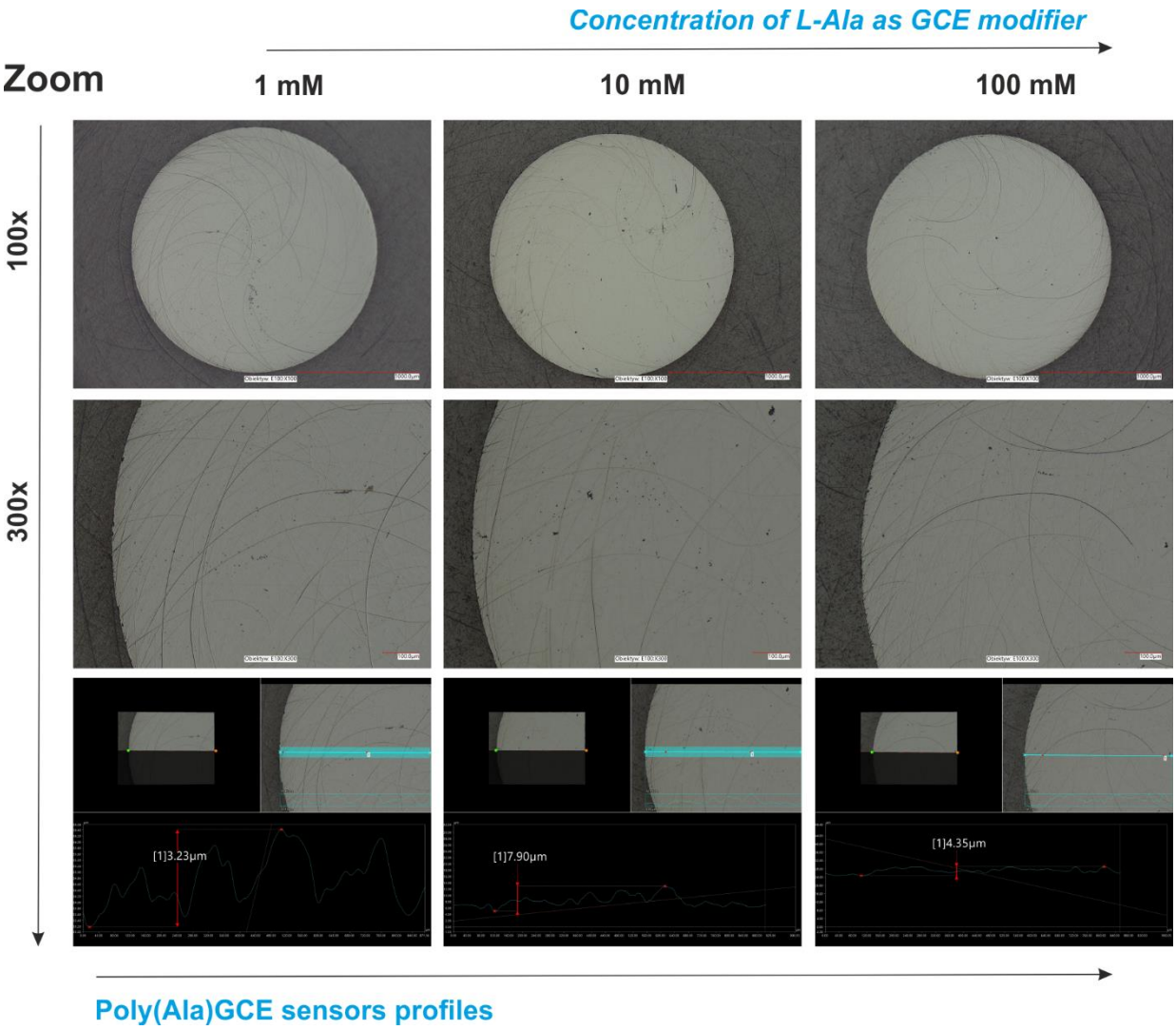

Figure S6. Microscopic imaging (two first rows) combined with the surface profiles of PAGCE sensors (third row).

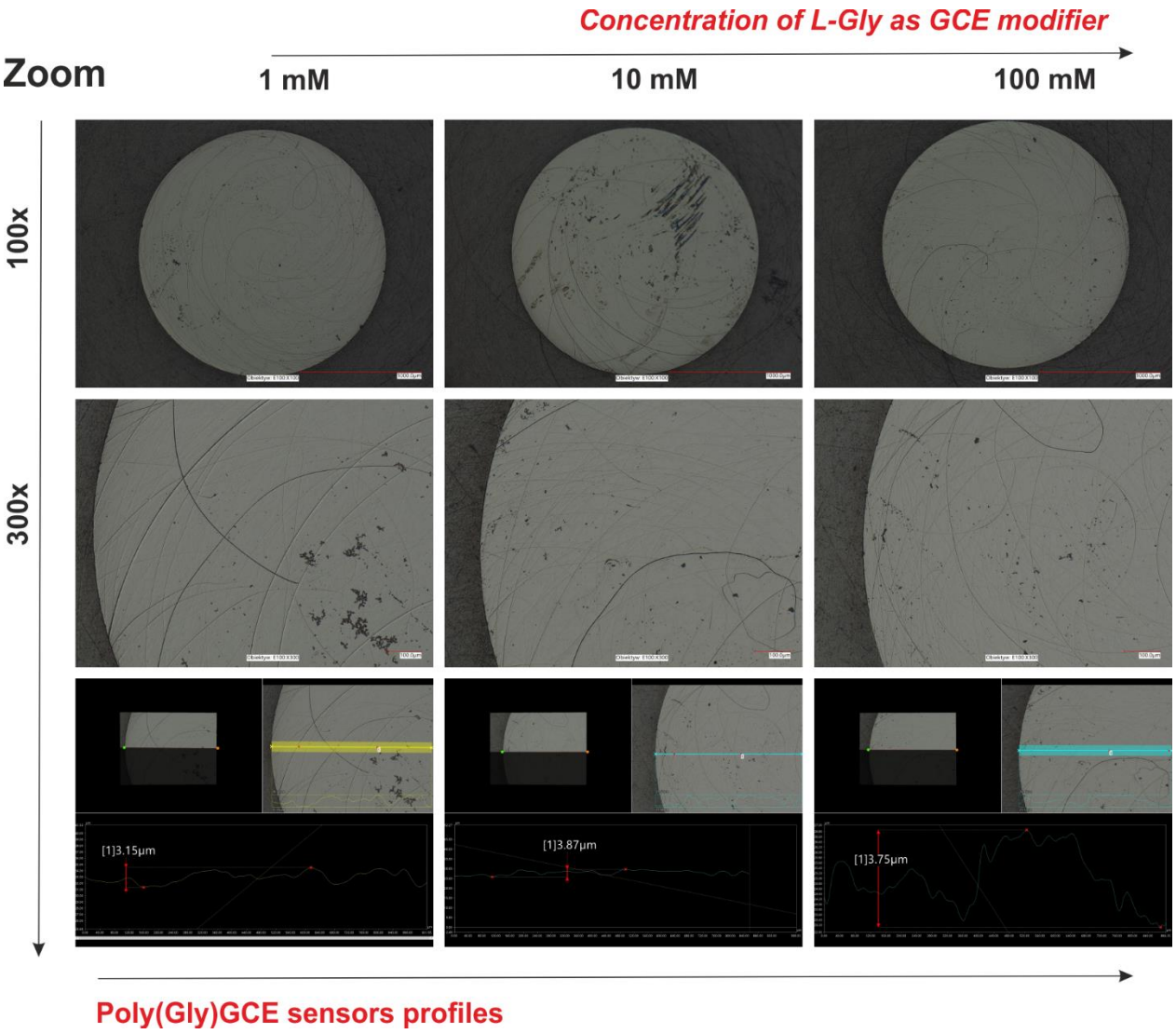

Figure S7. Microscopic imaging (two first rows) combined with the surface profiles of PGGCE sensors (third row).

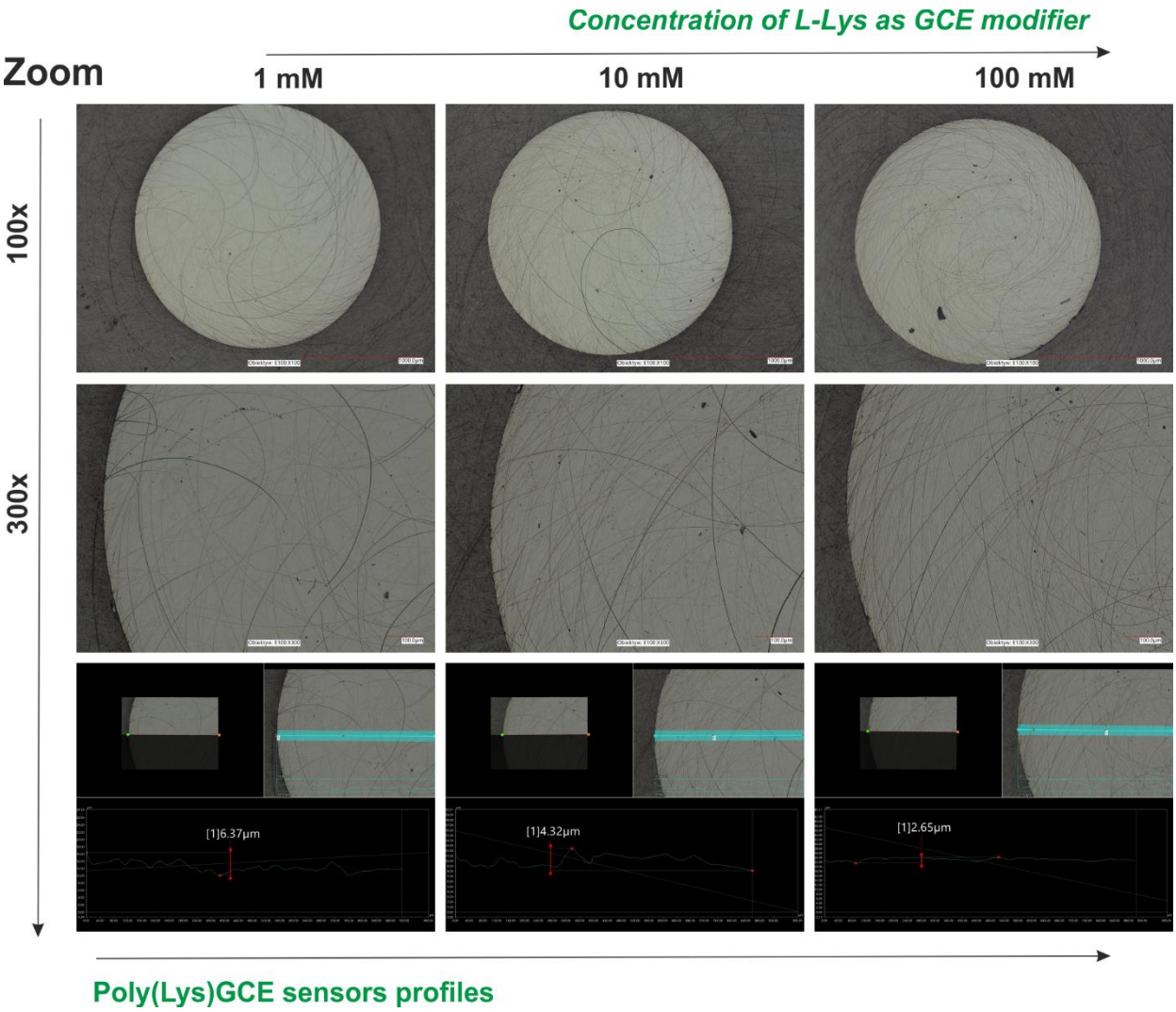

Figure S8. Microscopic imaging (two first rows) combined with the surface profiles of PLGCE sensors (third row).

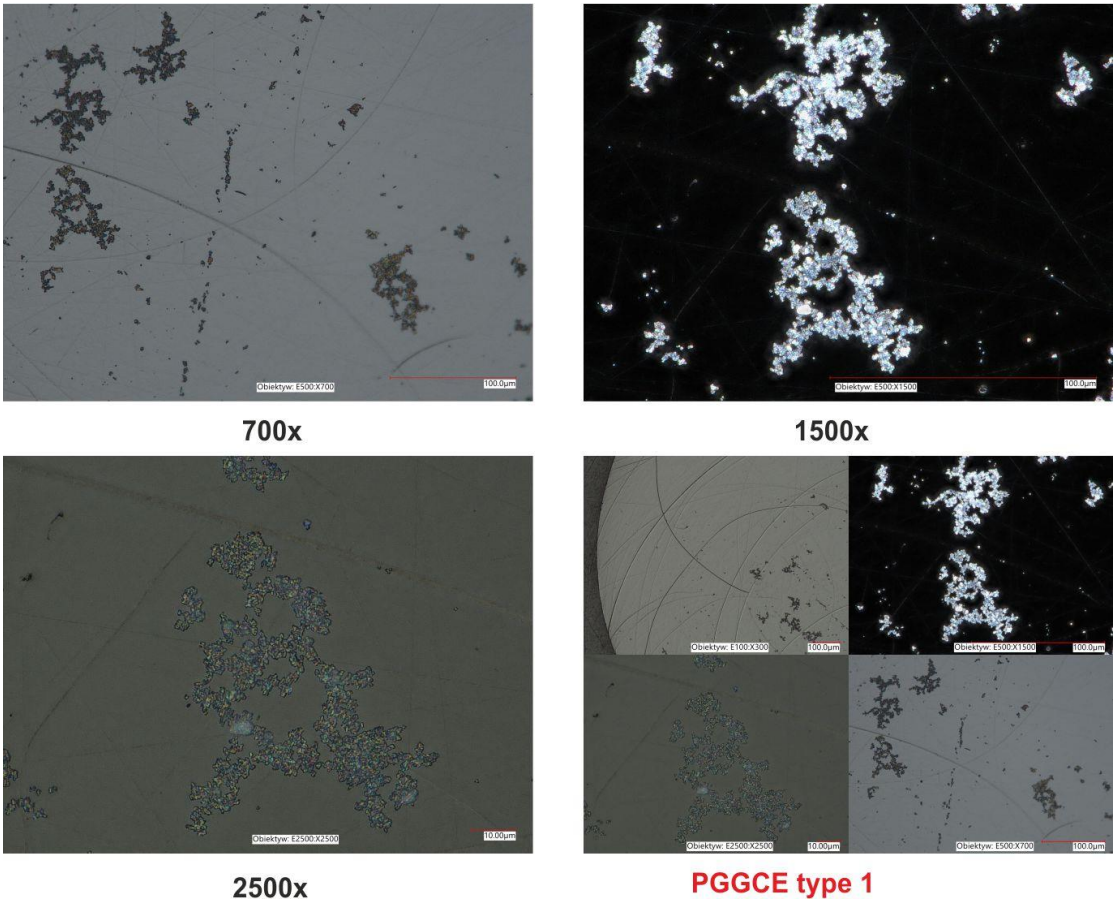

Figure S9. Images in magnification of the largest modification by volume - poly-L-glycine coating produced on the GCE surface, showing increased efficiency and sensitivity of detection of pyrazine derivatives in pharmaceuticals (*BZM*, *PZA*) and model systems (*PTCA*, *PAOX*).

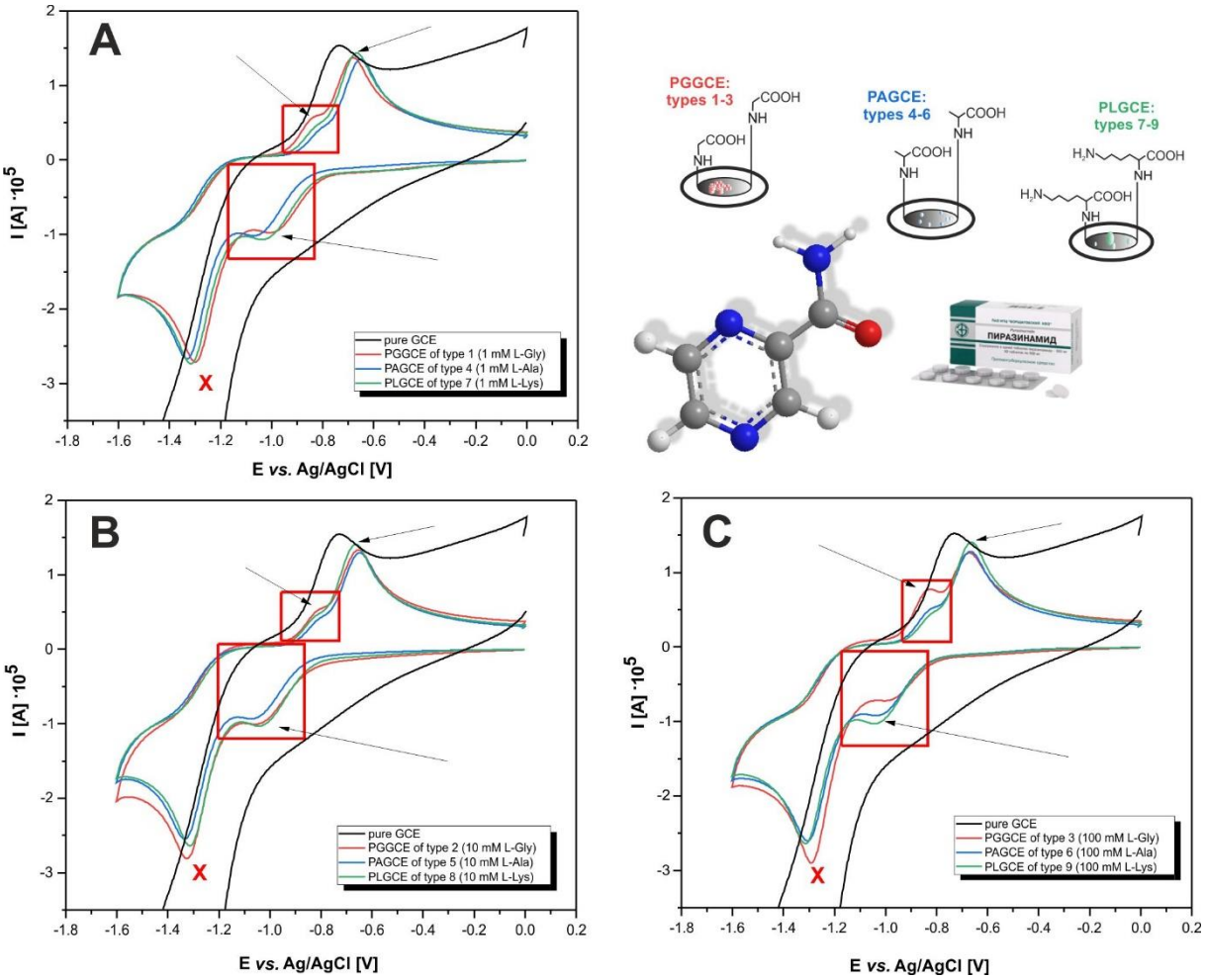

Figure S10. Cyclic voltammograms registered by 9 types of sensors were obtained for the *PZA* (2.00 mM solution) stoichiometric analyses which are commercially available and used as an anti-tuberculosis drug.

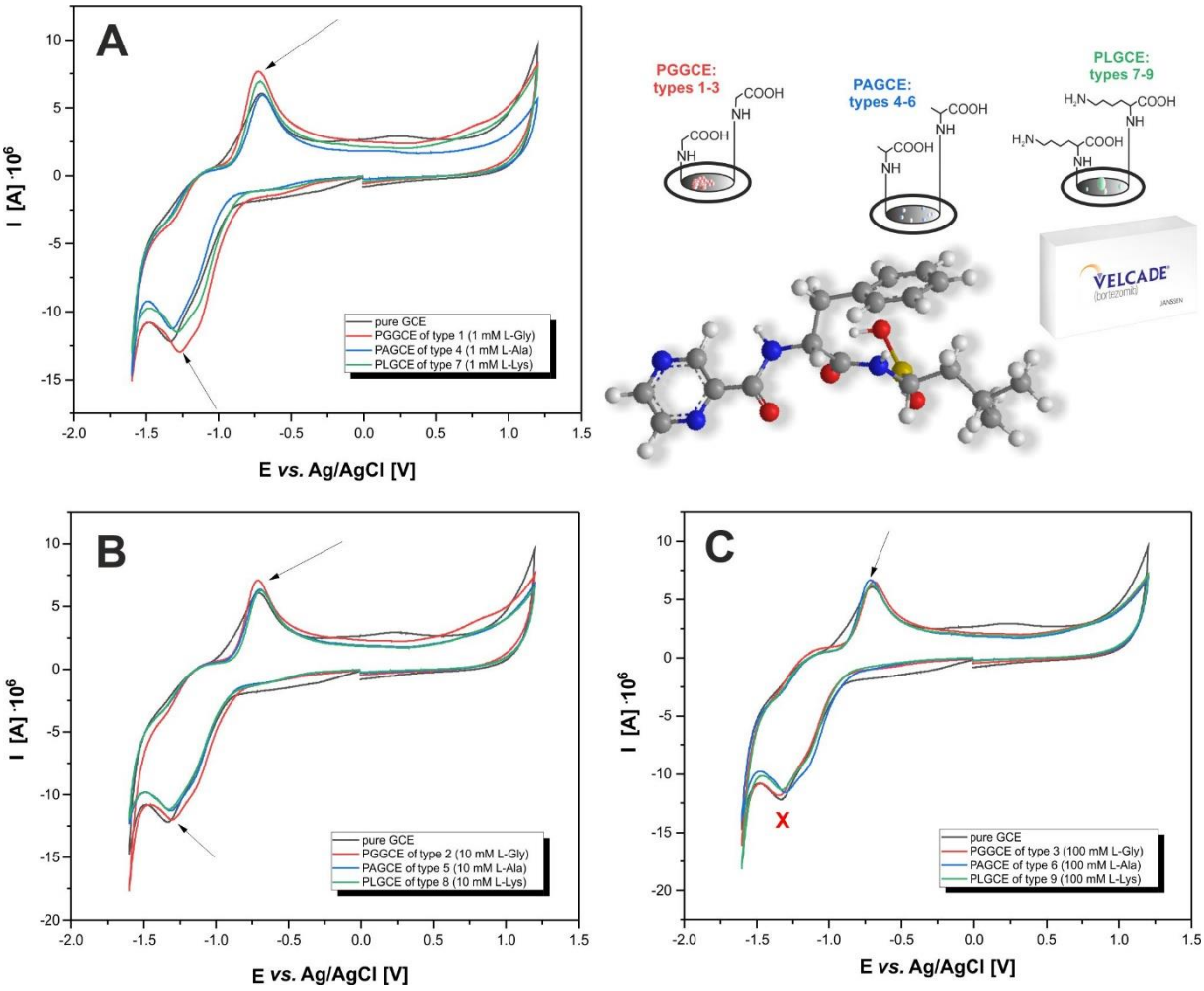

Figure S11. Cyclic voltammograms registered by 9 types of sensors obtained for the *BZM* (1.25 mM solution) stoichiometric analyses which are commercially available and used as an anticancer drug.

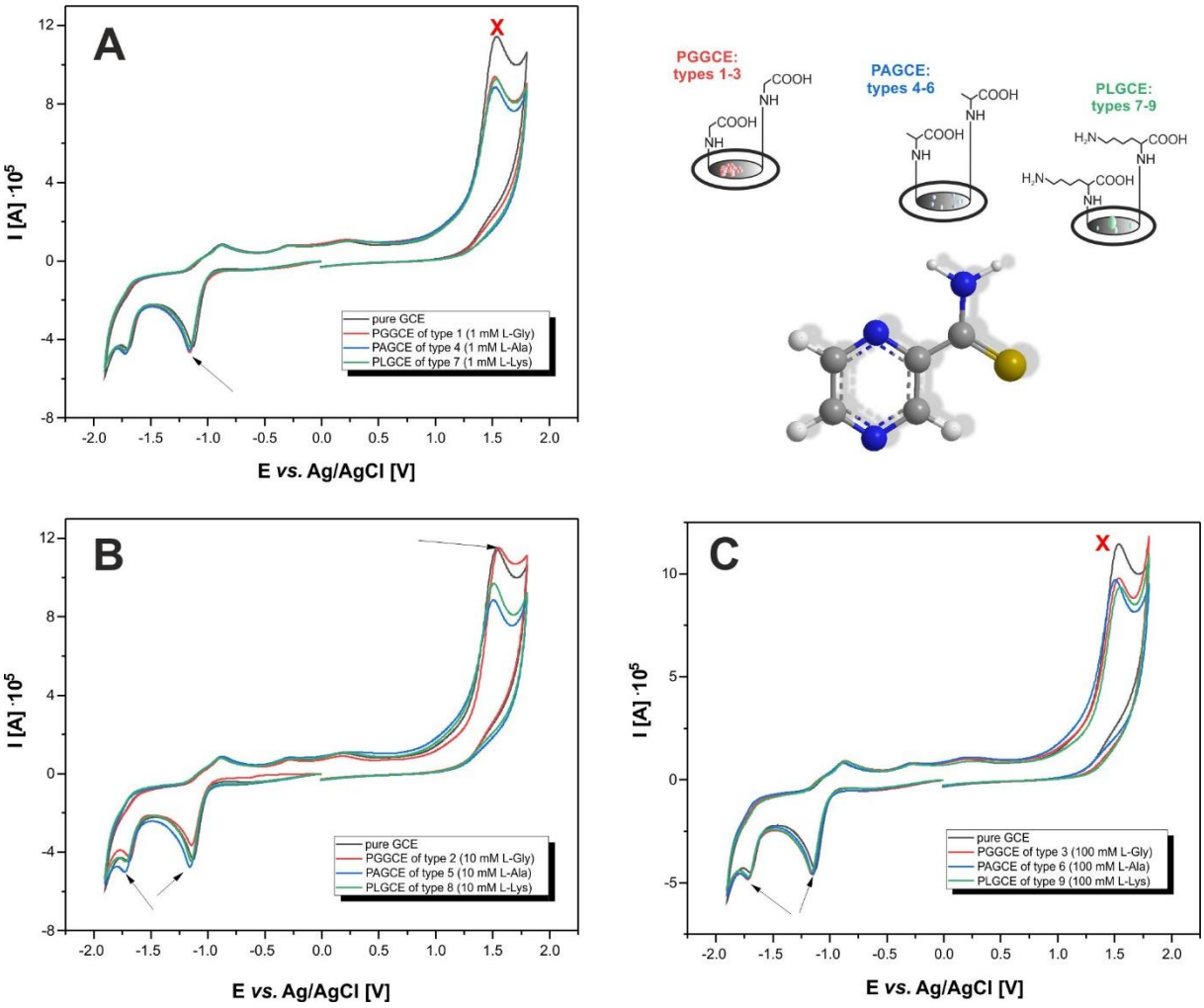

Figure S12. Cyclic voltammograms registered by 9 types of sensors were obtained for the *PTCA* (2.00 mM solution) stoichiometric analyses which show antimycotic properties [SR1].

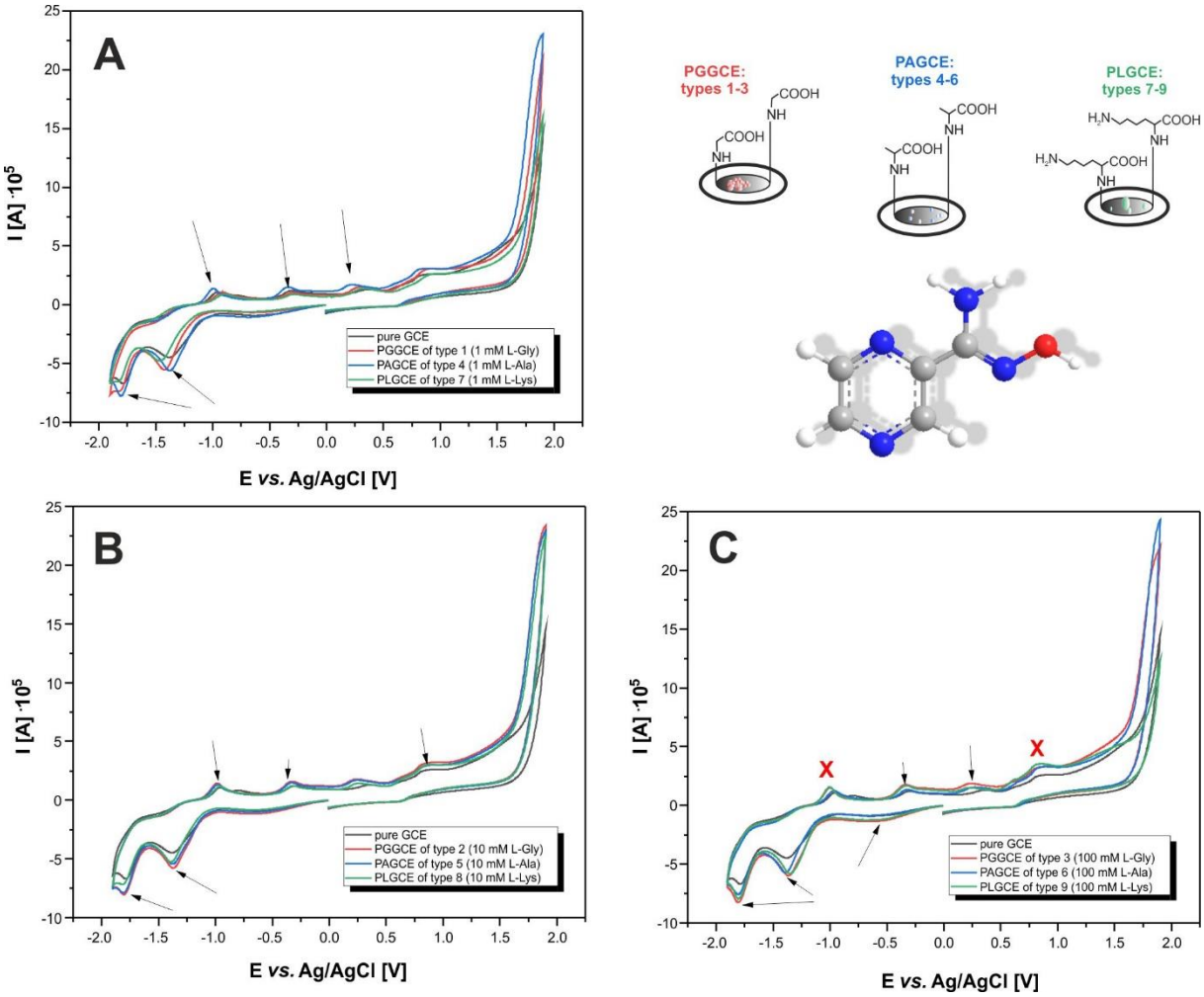

Figure S13. Cyclic voltammograms registered by 9 types of sensors were obtained for the *PAOX* (2.00 mM solution) stoichiometric analyses which show antimycotic properties with selective action against *Candida albicans* [SR2].

SUPPORTING REFERENCES

[SR1] A. Chylewska, A. Sikorski, M. Ogryzek, M. Makowski, Attractive S···π and π-π interactions in the pyrazine-2-thiocarboxamide structure: Experimental and computational studies in the context of crystal engineering and microbiological properties, *Journal of Molecular Structure*, 2016, 1105, 96-104, https://doi.org/10.1016/j.molstruc.2015.10.032

[SR2] A. Chylewska, PAOX, RSC Adv. 2016, A. Chylewska, M. Ogryzek, A. Głębocka, A. Sikorski, K. Turecka, E. D. Raczyńska, M. Makowski, Crystalline pyrazine-2-amidoxime isolated by diffusion method and its structural and behavioral analysis in the context of crystal engineering and microbiological activity, *RSC Adv.* 2016, 6, 64499 - 64512, DOI:10.1039/C6RA10537H